



## Photophysical studies of donor, acceptor substituted tetrahydrodibenzo[a,i]phenanthridines

Balijapalli Umamahesh <sup>a</sup>, Udayadasan Sathiskumar <sup>b</sup>, George Augustine <sup>c</sup>, Shanmugam Eswaramoorthi <sup>b,\*</sup>, Niraikulam Ayyadurai <sup>c</sup>, Kulathu Iyer Sathiyanarayanan <sup>a,\*\*</sup>

<sup>a</sup> School of Advanced Sciences, Vellore Institute of Technology University, Vellore, India

<sup>b</sup> Chemical Laboratory, CSIR-Central Leather Research Institute, Adyar, Chennai, 600020, India

<sup>c</sup> Biotechnology Division, CSIR-Central Leather Research Institute, Adyar, Chennai, 600020, India

### ARTICLE INFO

#### Article history:

Received 1 June 2016

Received in revised form

12 July 2016

Accepted 27 July 2016

Available online 31 July 2016

#### Keywords:

Phenanthridines

DNA intercalation

Photophysical studies

Fluorescence spectra

UV spectra

### ABSTRACT

Highly luminescent, 5-aryl-7,8,13,14-tetrahydrodibenzo[a,i]phenanthridines (THDPs) in Donor(D)- $\pi$ -Acceptor(A), A- $\pi$ -A, A- $\pi$ -A- $\pi$ -A<sub>1</sub> configurations were synthesized in good to moderate yields by simple, two step reactions. All the phenyl rings were found to be in near-coplanar configuration due to the enforced planarity by the ethylene bridge. As a result, efficient  $\pi$ -conjugation was maintained throughout the molecule. UV-visible absorption and fluorescence spectra of THDP became shifted to longer wavelengths upon substitution of different moieties at 5-Aryl position. A maximum of 200 nm red-shifted fluorescence with respect to parent compound was observed for the nitro substituent. However, tradeoffs in spectral shifts were noticed when two strongly electron withdrawing groups such as nitro and cyano groups were present simultaneously. Presence of one or more acceptors induced the intramolecular electron transfer processes, and the photophysical properties of THDP core was tuned by different substituents. Application of this fluorophore has also been demonstrated by means of DNA interaction studies.

© 2016 Elsevier Ltd. All rights reserved.

### 1. Introduction

Phenanthridine, a well-known polycyclic aromatic moiety has been the basic structural moiety for natural products, biologically and therapeutically active compounds and organic materials [1–5]. Indeed, phenanthridine derivatives such as ethidium bromide and propidium iodide have widely been explored for their role as fluorescent probe for biomolecules, owing to their high sensitivity towards hydrophobic and hydrophilic environments [6–12]. Considering their versatility, influence of heteroaryl ring fusion, and ease in substituting diverse functional groups, a variety of derivatives based on phenanthridine skeleton have been developed for different applications [13–15]. Most of the reports on phenanthridine derivatives have been studied for pharmaceutical and other biological applications [16,17]. Despite the rich  $\pi$ -electron

density with available positions for the introduction of functional groups to tune the electronic properties, only limited attention has been paid in understanding their electronic properties [18]. Indeed, molecules having donor- $\pi$ -acceptor configurations (D- $\pi$ -A) were found to show desired properties for multitude of applications ranging from organic electronics [19–21], fluorescent sensors [22–25], fluorescent probes for biological studies [26,27], and nonlinear optics [28]. The flexible nature of donor-acceptor systems offers exceptional tunability by diversifying the choice of electron donating and withdrawing substituents to produce the desired properties [29–34]. While polyaromatic compounds such as pyrene, fluorene, anthracene, and phenothiazine have been widely studied [35–37], not much work has been done on phenanthridine skeleton despite its synthetic advantage. In this work, we report the synthesis and photophysical studies of tetrahydrodibenzo[a,i]phenanthridine (**THDP**) substituted with electron donating and withdrawing groups. Recently, we have developed 5-aryl THDPs bearing fashionable functionalities [38,39]; however, the detailed fluorescence properties were not reported. The chromophoric unit resembles 2,3,5-triphenyl pyridines [39]. The presence of ethane

\* Corresponding author.

\*\* Corresponding author.

E-mail addresses: [moorthi@clri.res.in](mailto:moorthi@clri.res.in) (S. Eswaramoorthi), [sathiya\\_kuna@hotmail.com](mailto:sathiya_kuna@hotmail.com) (K.I. Sathiyanarayanan).

bridge ensures the coplanarity of all aromatic rings, thereby aiding the extensive  $\pi$ -electron delocalization throughout the molecule.

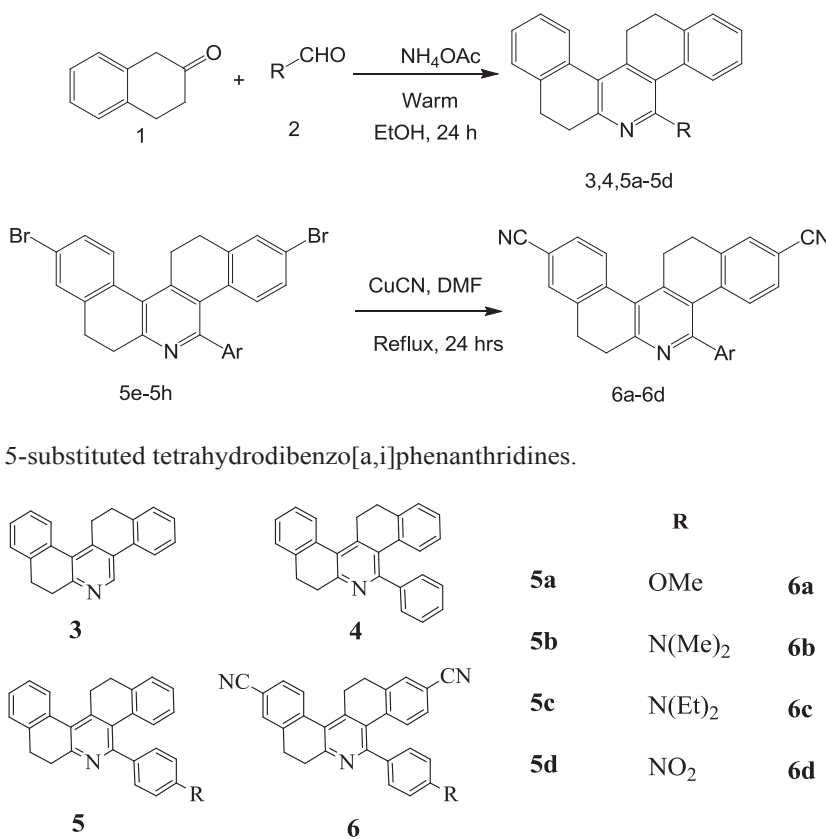
## 2. Results and discussion

The 7,8,13,14-tetrahydrodibenzo[a,i]phenanthridines (**Scheme 1**) were synthesized in a one-pot reaction in good yields, according to the reported procedure [38,39]. Similar protocol was followed for the synthesis of 2,10-dibromo-7,8,13,14 tetrahydrodibenzo[a,i] phenanthridines (**Br-THDP**, **5e–5h**) which was then converted to dicyano derivatives (**6a–6d**) in moderate yields using CuCN in DMF (**Scheme 1**). The compounds were characterized using FTIR,  $^1\text{H}$  NMR,  $^{13}\text{C}$  NMR, HRMS and single crystal X-ray crystallographic techniques. The single crystal of **5b** was grown in 1:1 ratio of ethanol and tetrahydrofuran mixture, and was then crystallized as triclinic system without solvation. The ORTEP diagram of **5b** given in **Fig. 1** indicates that the dihedral angle 32.12° respectively, is in fact smaller than that of the simple biphenyl ( $44 \pm 1.2^\circ$ ). The significant decrease in dihedral between the aromatic units viz. C3C8C9C21, C19C20C22C23, and C10C19C18C13 was measured to be 24.69°, 37.30° and the angle was attributed to the enforced coplanarity caused by ethylene bridge that connected 2, 2' positions of both the phenyl groups.

The UV–Visible absorption spectra of the parent compound **3**, given in **Fig. 2**, shows two well-resolved peaks in acetonitrile solvent with the peak maxima at 294, 322 nm. The fluorescence emission having mirror image relationship with lowest energy absorption band was observed at 358 nm. While going from **3** to **4**, by introducing the phenyl group at the 5th position of tetrahydrodibenzo[a,i]phenanthridine ring, absorption spectra became blue shifted by 14 nm and the emission maximum was found to be slightly red shifted. Overall Stokes shift for **3** and **4** corresponded to

3123, 4690  $\text{cm}^{-1}$  respectively, which is an indication of stronger structural perturbations between the ground and excited state geometries in presence of 5–phenyl substituent. Indeed, substitution of 5-phenyl (**5a–5d**) and cyano groups on phenanthridine (**6a–6d**) respectively in D– $\pi$ –A, A– $\pi$ –D– $\pi$ –A format significantly altered the absorption and emission spectra characteristic to the nature of the substituents, as shown in **Fig. 2**. The spectral properties, summarized in **Table 1** and **Fig. 2**, suggest that electron donating OMe (**5a**), N(Me)<sub>2</sub> (**5b**), N(Et)<sub>2</sub> (**5c**) and electron withdrawing NO<sub>2</sub> (**5d**) groups in 5–phenyl ring cause red-shifted absorption and fluorescence respectively by 10–52 nm, and 57–201 nm compared to **4**. Surprisingly, **5d** with nitro substitution showed nearly 200 nm red-shifted ( $\lambda_{\text{fl}} = 560 \text{ nm}$ ) fluorescence with respect to the parent compound **4** ( $\lambda_{\text{fl}} = 360 \text{ nm}$ ). It should be noted that the spectral shift was larger in magnitude for fluorescence than that of the absorption bands. The Stokes shift value, calculated from the lowest energy absorption and the highest energy emission, was found to be 4690, 7110, 7560, 6180, 11130  $\text{cm}^{-1}$  respectively for **4**, **5a**, **5b**, **5c**, and **5d**. The larger Stokes shift values and the significant substituent effect on fluorescence revealed strong intramolecular charge transfer interactions between the phenanthridine and substituted 5-phenyl moieties. Indeed, combinations of strong electron donating, –NR<sub>2</sub> and electron accepting, cyano group further red-shifted emission at least by 44 nm in **6b**, **6c** when compared to **5b**, **5c**. On the other hand, the compound with electron withdrawing nitro substituent, **6d** in A– $\pi$ –D–( $\pi$ –A)– $\pi$ –A<sub>1</sub> format shows fluorescence at 518 nm, which is blue shifted by 43 nm when compared to **5d**. These features suggest that the photophysical properties could be altered efficiently by the judicious choice of donor and acceptor combinations.

The fluorescence quantum yields ( $\phi_{\text{fl}}$ ) measured with reference to quinine sulphate in 0.5 M H<sub>2</sub>SO<sub>4</sub> is given in **Table 1**. It reveals that



**Scheme 1.** Synthetic route for D– $\pi$ –A, A– $\pi$ –A, A– $\pi$ –A– $\pi$ –A<sub>1</sub> phenanthridines.

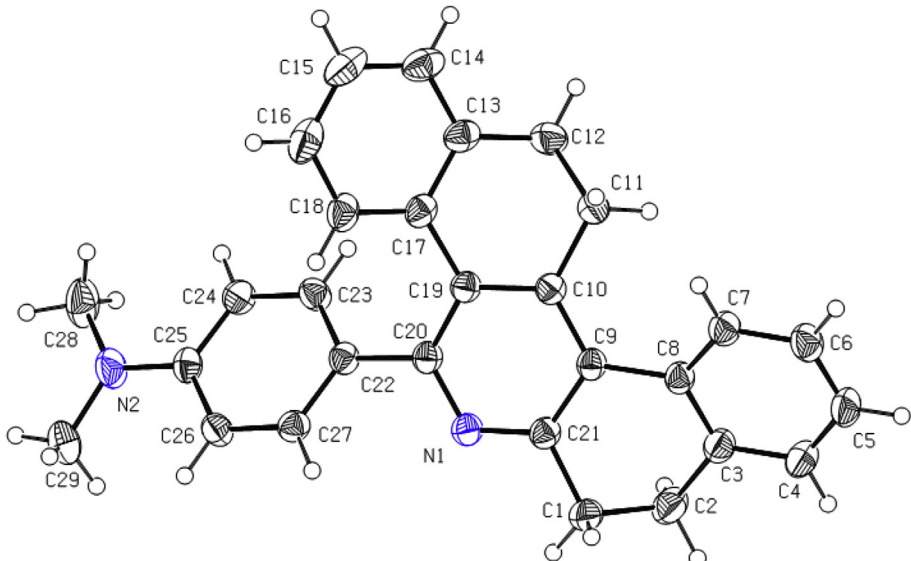


**Fig. 1.** ORTEP diagram of compound **5b** with ellipsoid shown at the 40% contour percent probability level (CCDC-1446308).

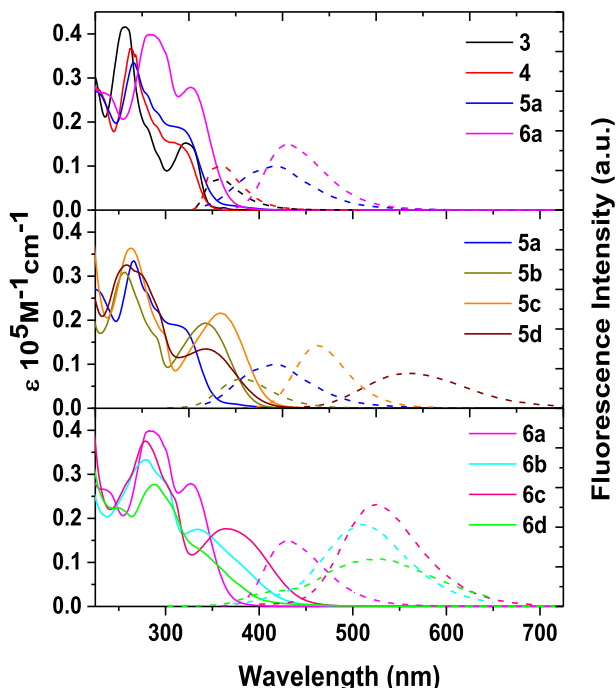


**Fig. 2.** UV–Visible absorption (—) and fluorescence (—) spectra of compounds **3**, **4**, **5a**–**5d** and **6a**–**6d** measured in acetonitrile solvent.

the  $\phi_f$  becomes enhanced, by the factor of 180, 320 times respectively by  $-\text{N}(\text{CH}_3)_2$  (**5b**, **6b**) and  $-\text{N}(\text{C}_2\text{H}_5)_2$  (**5c**, **6c**) when compared to the parent compound **4**. To get more insights, fluorescence lifetimes of the samples in solution state were measured using time correlated single photon counting technique by exciting the samples at 375 nm. The decay profiles of the samples monitored at respective emission wavelength and the corresponding data are summarized in Table 1 (see the Supporting information, Fig. S1). The fluorescence lifetime of **4**, **5a**, **5b**, **5c**, and **5d** was measured to be 1.39, 1.44, 1.19, 0.68, 2.05 ns respectively in acetonitrile solvent. Longer fluorescence lifetimes were observed for **6b**, **6c** with A– $\pi$ –D– $\pi$ –D<sub>1</sub> system than that of the corresponding D-A systems such as compounds **5b** and **5c**. This feature would have originated

from the intramolecular charge transfer (ICT) interactions between the electron rich and deficient groups. Solvent polarity induced red-shifted fluorescence was observed for all the compounds, however to a different extent, which indicates the ICT interactions. Representative fluorescence spectra of compounds **5b**, **5c**, **6b**, and **6c** in solvents of different polarity are given in Fig. 3, and the data are compiled in Table 2 (see the Supporting information, Fig. S2). The fluorescence spectrum became gradually red-shifted with an increase in solvent polarity due to the larger, solvent polarity induced dipole moment changes between the ground and excited states. It should be noted that the introduction of electron withdrawing cyano group in the phenanthridine moiety induced significantly enhanced charge transfer character, as can be seen from large spectral shifts for **6b**, **6c** than **5b** and **5c**. This feature can be ascribed to the presence of both-electron donating and withdrawing groups connected through  $\pi$ -conjugation. Indeed, the magnitude of ICT character could also be understood from the slope value of the Lippert-Mataga<sup>13</sup> plot, an indication of the difference in stabilization of ICT states by the substituents (see the Supporting information, Fig. S3). For instance, electron donating groups  $-\text{NR}_2$ , exhibited larger slope value  $\sim 9000 \text{ cm}^{-1}$  while that of  $-\text{OCH}_3$  was calculated to be  $3650 \text{ cm}^{-1}$ . Further, the lifetime of the parent compound **3** was found to remain constant irrespective of the solvent polarity, the donor-acceptor substituted one show pronounced enhancement in fluorescence lifetime in polar solvents. The corresponding change in fluorescence lifetime spectra with respect to solvent polarity for compounds **5b**, **5c**, **6b** and **6c** is depicted in Fig. 4. This feature can be ascribed to the emission from the charge transferred state. Further, it can be expected that the N,N-dialkylamino groups would form highly conjugated quinonoid like charge transferred state having intervening double bonds between the phenyl rings as depicted in Scheme 2.

Interestingly, the presence of two cyano groups in **6** offers possibly, two different CT states having *ortho* and or *para* quinonoid structures. It is really difficult to discriminate between the CT states experimentally, as both of them are expected to show solvatochromism in fluorescence. To explore this further, molecular orbitals were calculated at B3LYP/6-31G level using Gaussian 03 software [40,41] using the geometry optimized structure at the same level of theory and corresponding molecular orbitals was given in Fig. 5 (see the Supporting information, Fig. S4). While the

**Table 1**

Photophysical properties of tetrahydrodibenzophenanthridines in acetonitrile solvent.

Comp	$\lambda_{\text{abs}}$ nm ( $\epsilon \cdot 10^{-1} \text{ M}^{-1} \text{ cm}^{-1}$ )	$\lambda_{\text{fl}}$ nm	Stokes shift cm <sup>-1</sup>	<sup>a</sup> $\Phi_{\text{fl}}$	<sup>b</sup> $\tau_{\text{fl}}$ ns	$K_r [10^8 \text{ s}^{-1}]$	$K_{\text{nr}} [10^8 \text{ s}^{-1}]$
<b>3</b>	257 (0.42), 283 (0.18), 294 (0.12), 322 (0.16)	358	3123	0.690	3.66	0.189	0.085
<b>4</b>	263 (0.36), 291 (0.18), 308 (0.15)	360	4690	0.001	1.39	0.001	0.719
<b>5a</b>	266 (0.34), 282 (0.26), 293 (0.22), 318 (0.19)	417	7110	0.007	1.44	0.005	0.709
<b>5b</b>	255 (0.31), 292 (0.16), 342 (0.20)	463	7560	0.182	1.19	0.153	0.688
<b>5c</b>	263 (0.37), 299 (0.17), 360 (0.22)	463	6180	0.351	0.68	0.516	0.954
<b>5d</b>	258 (0.33), 274 (0.30), 344 (0.14)	561	11130	0.037	2.05	0.018	0.470
<b>6a</b>	237 (0.27), 283 (0.40), 328 (0.28)	432	7220	0.036	$\leq \text{IRF}^{\text{c}}$	—	—
<b>6b</b>	279 (0.34), 302 (0.28), 337 (0.18)	507	9350	0.191	3.56	0.054	0.227
<b>6c</b>	278 (0.38), 310 (0.25), 366 (0.18)	525	8730	0.339	3.77	0.090	0.175
<b>6d</b>	251 (0.22), 288 (0.28), 345 (0.12)	518	9610	0.039	1.11	0.035	0.862

<sup>a</sup> Fluorescence quantum yields were measured with reference to quinine sulfate  $\Phi_{\text{fl}} = 0.546$  in  $\text{H}_2\text{SO}_4$  0.5 M,  $\lambda_{\text{fl}} = 310$  nm.

<sup>b</sup> The decay profiles were monitored at respective fluorescence maximum.

<sup>c</sup> IRF-Instrument response function.

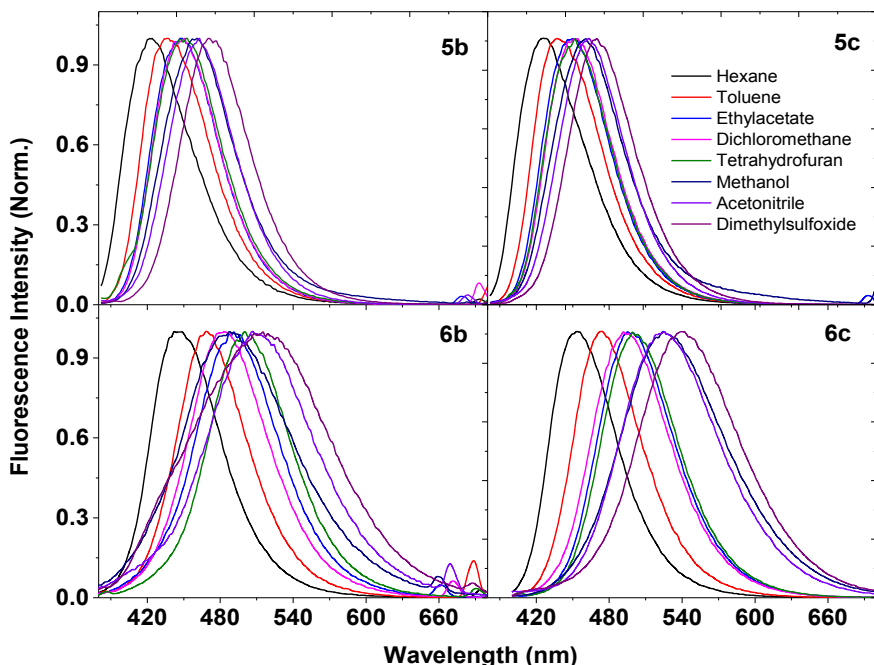


Fig. 3. Fluorescence spectra for the compounds **5b**, **5c**, **6b** and **6c** measured in solvents of variable polarities.

electron donating groups destabilized the highest occupied molecular orbitals (HOMO) at least by 0.54 eV with respect to parent compound, the lowest unoccupied molecular orbital (LUMO) did not show any significant changes with substitution. On the contrary, the HOMO was stabilized by 0.18, 0.80 eV respectively for **5d** and **6d** when compared to **4**. Overall decrease in HOMO-LUMO gap was observed when both the donor-acceptor moieties were present. The theoretically calculated HOMO-LUMO values were in good agreement with the experimental values (see Table 3). The electron density, mainly localized on 5-phenyl substituent, became redistributed in phenanthridine core during transition from HOMO to LUMO. In contrast, compound **5d** with nitro substituent showed complete shift in electron density from phenanthridine core to nitrophenyl ring during transition from HOMO to LUMO orbital. The frontier orbitals did not distinguish the *ortho* and *para* quinonoid forms and hence both might contribute to the charge transferred state. Similar behaviour was observed for the compound **6d** that had both nitro and cyano groups. Among them, nitro group was found to be strong acceptor.

To evaluate the applications of THDP derivatives and the role of substituents, labelling and detection of double strand DNA

(dsDNA), which is a powerful method for many molecular biology experiments, was carried out. Hence, the intercalating efficiency of compound **3** to **6d** was investigated with bacterial genomic DNA, PCR product, and DNA ladders. Efficient separations and reproducibility of migration time of dsDNA fragments were obtained for all the compounds. The linear range and sharp intensity of dsDNA ladder mix was comparable with the commonly used ethidium bromide. Further, the PCR product and genomic DNA interaction indicated that detection, or intercalating efficiency of all the compounds were high and well suited for DNA electrophoresis or other dsDNA quantification analysis (Fig. 6). On the other hand, it has been well documented that DNA intercalating agents are not only used for labelling studies but also plays an essential role in developing several clinically used anticancer and antibiotic drugs. In this connection much attention has been focused to rational designing, new natural products and synthesis of potential synthetic and efficient DNA-targeting cytotoxic intercalators. Our results on compound **3** to **6d** intercalating efficiency encourage us to believe that it can also be used as a potential drug for cancer therapy. However, to prove our state of concept, further studies may be needed for better understanding of the DNA intercalating

**Table 2**

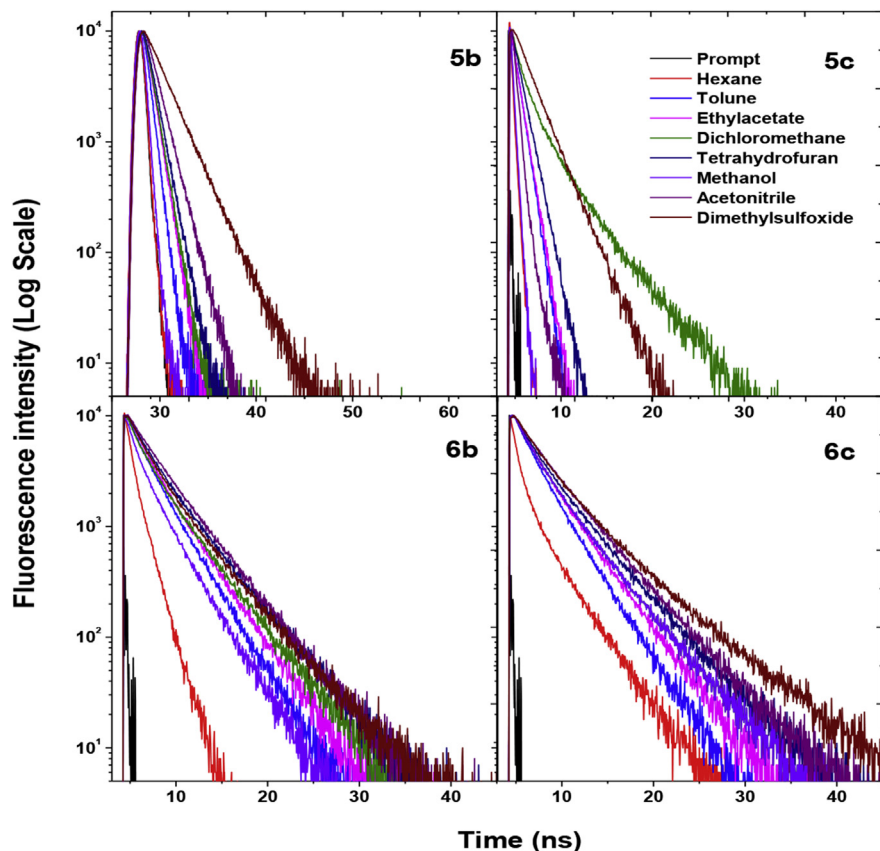
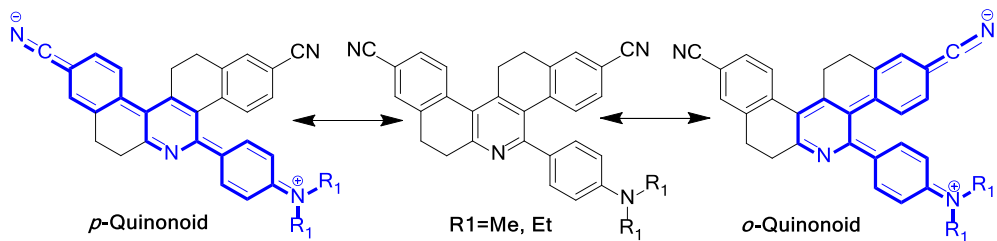
Optical data measured in different solvents.

Compound	Solvent	$\lambda_{\text{abs.}}$ nm	$\lambda_{\text{fl.}}$ nm	Stoke's shift cm <sup>-1</sup>	$\Phi_{\text{fl}}$	$\tau_{\text{fl}}$ ns	$K_r [10^8 \text{ s}^{-1}]$	$K_{\text{nr}} [10^8 \text{ s}^{-1}]$
<b>3</b>	Hexane	259, 282, 294, 323	358	3027	0.149	3.14	0.047	0.271
	Toluene	295, 323	362	3335	0.513	3.24	0.158	0.150
	Dichloromethane	266, 293, 322	363	3508	0.291	3.67	0.079	0.193
	Tetrahydrofuran	256, 283, 295, 323	356	2870	0.665	3.33	0.199	0.101
	Ethyl acetate	274, 285, 315	358	3813	0.567	3.46	0.163	0.125
	Methanol	261, 281, 294, 324	361	3163	0.141	3.96	0.035	0.217
	Acetonitrile	255, 282, 293, 322	358	3123	0.690	3.66	0.188	0.084
<b>4</b>	Dimethylsulfoxide	263, 285, 297, 325	360	2991	0.227	3.88	0.058	0.199
	Hexane	264, 291, 309	363	4814	0.001	0.26	0.004	3.842
	Toluene	312	361	4350	0.002	<IRF	—	—
	Dichloromethane	266, 294, 318	361	3746	0.010	<IRF	—	—
	Tetrahydrofuran	266, 293, 313	362	4325	0.009	<IRF	—	—
	Ethyl acetate	265, 292, 314	359	3992	0.030	<IRF	—	—
	Methanol	265, 292, 318	362	3822	0.002	0.29	0.007	3.441
<b>5a</b>	Acetonitrile	263, 291, 308	360	4690	0.001	1.39	0.001	0.719
	Dimethylsulfoxide	266, 294, 316	360	3868	0.003	0.51	0.006	1.955
	Hexane	268, 282, 294, 322	389, 408	6546	0.015	0.45	0.033	2.188
	Toluene	294, 320	419	7384	0.011	<IRF	—	—
	Dichloromethane	267, 282, 322	424	7471	0.051	0.25	0.204	3.796
	Tetrahydrofuran	267, 280, 294, 322	420	7246	0.027	<IRF	—	—
	Ethyl acetate	258, 273, 285, 310	425	8729	0.362	<IRF	—	—
<b>5b</b>	Methanol	266, 280, 291, 318	405, 428	8082	0.017	0.36	0.047	2.730
	Acetonitrile	267, 282, 295, 321	416	7114	0.007	1.44	0.004	0.689
	Dimethylsulfoxide	268, 282, 294, 320	415	7154	0.012	0.67	0.017	1.474
	Hexane	255, 273, 289, 346	422	5205	0.050	<IRF	—	—
	Toluene	292, 351	436	5554	0.112	0.27	0.414	3.288
	Dichloromethane	258, 292, 347	449	6547	0.269	0.80	0.336	0.913
	Tetrahydrofuran	253, 291, 348	452	6612	0.396	0.91	0.435	0.663
<b>5c</b>	Ethyl acetate	283, 338	449	7314	0.164	0.75	0.218	1.114
	Methanol	256, 291, 342	460	7501	0.080	<IRF	—	—
	Acetonitrile	255, 290, 343	463	7556	0.182	1.19	0.152	0.687
	Dimethylsulfoxide	293, 350	470	7295	0.215	2.13	0.100	0.368
	Hexane	259, 291, 355	425	4640	0.112	<IRF	—	—
	Toluene	292, 359	437	4972	0.123	0.80	0.154	1.096
	Dichloromethane	262, 293, 357	449	5739	0.446	1.22	0.366	0.454
<b>5d</b>	Tetrahydrofuran	255, 292, 357	452	5887	0.437	1.06	0.412	0.531
	Ethyl acetate	283, 346	449	6630	0.321	0.85	0.378	0.799
	Methanol	261, 291, 352	461	6717	0.106	0.68	0.156	1.315
	Acetonitrile	259, 298, 360	463	6180	0.351	0.68	0.516	0.954
	Dimethylsulfoxide	263, 292, 361	470	6424	0.494	1.02	0.484	0.496
	Hexane	251, 276, 339	—	—	—	—	—	—
	Toluene	294, 351	—	—	—	—	—	—
<b>6a</b>	Dichloromethane	261, 278, 353	540	9810	0.059	1.13	0.052	0.832
	Tetrahydrofuran	250, 277, 350	—	—	—	—	—	—
	Ethyl acetate	267, 339	—	—	—	—	—	—
	Methanol	258, 270, 334	—	—	—	—	—	—
	Acetonitrile	255, 274, 345	560	11128	0.037	2.05	0.018	0.470
	Dimethylsulfoxide	266, 352	563	10647	0.085	1.09	0.078	0.839
	Hexane	245, 282, 336	420	5952	0.048	<IRF	—	—
<b>6b</b>	Toluene	295, 334	422	6243	0.007	<IRF	—	—
	Dichloromethane	286, 333	425	6501	0.066	<IRF	—	—
	Tetrahydrofuran	287, 332	426	6646	0.050	<IRF	—	—
	Ethyl acetate	276, 324	423	7224	0.188	<IRF	—	—
	Methanol	282, 326	426	7201	0.048	<IRF	—	—
	Acetonitrile	283, 329	430	7139	0.036	<IRF	—	—
	Dimethylsulfoxide	293, 331	435	7223	0.039	0.27	0.144	3.559
<b>6c</b>	Hexane	270, 348	444	6213	0.193	0.60	0.322	1.345
	Toluene	301, 344	469	7748	0.125	1.40	0.089	0.625
	Dichloromethane	281, 303, 342	482	8493	0.573	1.68	0.341	0.254
	Tetrahydrofuran	278, 303, 344	500	9070	0.379	2.93	0.129	0.212
	Ethyl acetate	271, 293, 333	489	9580	0.183	2.55	0.072	0.320
	Methanol	279, 332	488	9629	0.116	1.13	0.103	0.782
	Acetonitrile	256, 290, 343	505	9353	0.191	3.56	0.054	0.227
<b>6c</b>	Dimethylsulfoxide	282, 304, 344	516	9690	0.214	1.79	0.200	0.734
	Hexane	273, 302, 369	455	5122	0.209	1.07	0.195	0.739
	Toluene	304, 368	474	6077	0.427	1.48	0.289	0.387
	Dichloromethane	274, 305, 363	493	7264	0.842	1.53	0.550	0.103
	Tetrahydrofuran	273, 303, 364	499	7432	0.740	3.19	0.232	0.082
	Ethyl acetate	264, 296, 358	494	7690	0.565	2.74	0.206	0.159
	Methanol	273, 360	525	8730	0.148	1.77	0.084	0.481
	Acetonitrile	260, 298, 360	525	8730	0.339	3.77	0.090	0.175
	Dimethylsulfoxide	275, 306, 375	541	8182	0.470	2.42	0.194	0.219

(continued on next page)

**Table 2** (continued)

Compound	Solvent	$\lambda_{\text{abs}}$ , nm	$\lambda_{\text{fl}}$ , nm	Stoke's shift cm <sup>-1</sup>	$\Phi_{\text{fl}}$	$\tau_{\text{fl}}$ ns	$K_f$ [10 <sup>8</sup> s <sup>-1</sup> ]	$K_{\text{nr}}$ [10 <sup>8</sup> s <sup>-1</sup> ]
<b>6d</b>	Hexane	280, 350	413	4358	0.300	0.64	0.515	1.046
	Toluene	299, 343	443	6581	0.014	0.88	0.015	1.120
	Dichloromethane	284, 345	475	7933	0.292	1.46	0.200	0.484
	Tetrahydrofuran	283, 331	469	8890	0.043	1.36	0.031	0.703
	Ethyl acetate	274, 329	452	8271	0.015	1.11	0.013	0.887
	Methanol	282, 333	475	8977	0.010	0.84	0.011	1.178
	Acetonitrile	288, 349	525	9606	0.039	1.11	0.035	0.865
	Dimethylsulfoxide	282, 360	510	8170	0.073	1.24	0.058	0.747

**Fig. 4.** Fluorescence lifetime decay profile for the compounds **5b**, **5c**, **6b** and **6c** measured in solvents of variable polarities.**Scheme 2.** Feasible charge transfer states in A- $\pi$ -D system (compounds **6b** and **6c**).

mechanisms and cytotoxicity efficiency, which will facilitate the improvement in selectivity to become a potent DNA intercalator. Current studies, including understanding the mechanism along with those lines of research, are on-going in our laboratories.

### 3. Conclusions

In conclusion, we have developed tetrahydrodibenzo[a,i]

phenanthridines with fashionable useful functionalities and exceptional fluorescence properties. The electronic properties of phenanthridine were significantly altered in a desired way by introducing suitable substituents. The combinations of electron donating and withdrawing groups as well as two different electron withdrawing groups were also found to induce the intramolecular charge transfer interactions, however, to a different extent. Indeed, the intercalating efficiency of all these compounds is also

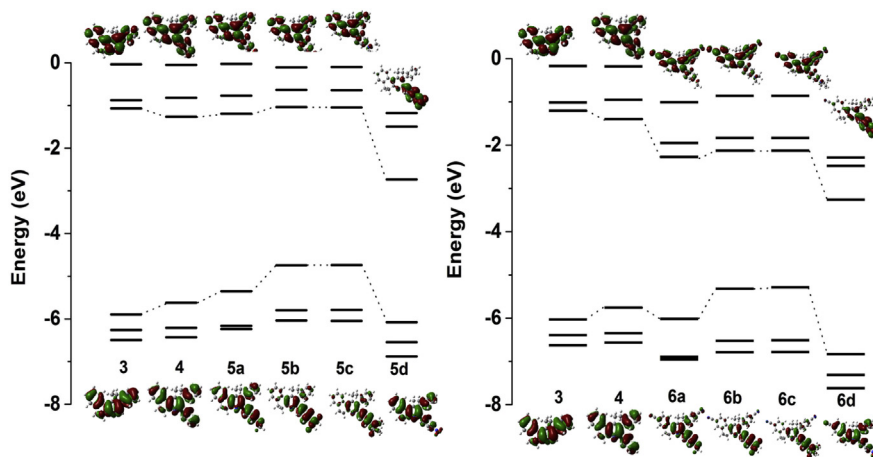


**Fig. 5.** Frontier molecular orbitals of phenanthridines at B3LYP/6-31G level of theory using Gaussian 03 software.

**Table 3**  
Theoretical and electrochemical properties.

Compound	<sup>a</sup> E <sub>ox</sub> (V)	<sup>a</sup> E <sub>red</sub> (V)	<sup>b</sup> E <sub>HOMO</sub> (eV)	<sup>b</sup> E <sub>LUMO</sub> (eV)	<sup>c</sup> E <sub>g</sub> (eV)	<sup>d</sup> HOMO (eV)	<sup>d</sup> LUMO (eV)	<sup>e</sup> E <sub>g</sub> (eV)	<sup>f</sup> ΔE <sub>00</sub> (eV)
<b>3</b>	1.68	-1.51	-6.08	-2.89	3.19	-5.89648	-1.06751	4.83	3.58
<b>4</b>	1.64	-1.52	-6.04	-2.88	3.16	-5.89644	-1.06750	4.82	3.57
<b>5a</b>	1.52	-1.87	-5.92	-2.53	3.39	-5.35470	-1.19513	4.16	3.51
<b>5b</b>	1.45	-1.89	-5.85	-2.51	3.34	-4.74162	-1.03431	3.71	3.16
<b>5c</b>	1.25	-1.93	-5.65	-2.47	3.18	-4.73944	-1.04275	3.69	3.03
<b>5d</b>	1.75	-1.37	-6.15	-3.03	3.12	-6.07853	-2.73477	3.34	3.06
<b>6a</b>	1.64	-1.75	-6.04	-2.65	3.39	-5.88124	-2.13665	3.74	3.39
<b>6b</b>	0.99	-1.82	-5.39	-2.58	2.81	-5.18408	-1.99407	3.18	2.90
<b>6c</b>	0.97	-1.80	-5.37	-2.60	2.77	-5.15360	-1.99407	3.16	2.80
<b>6d</b>	1.67	-1.40	-6.07	-3.00	3.07	-6.69569	-3.12389	3.57	3.08

<sup>a</sup> The redox potential of compounds obtained from cyclic voltammetry using glassy carbon as working electrode with reference to Fc/Fc + couple. 0.1 M Tetrabutylammonium perchlorate was used as a supporting electrolyte.

<sup>b</sup> E<sub>HOMO/LUMO</sub> HOMO and LUMO energy levels calculated from the redox potentials.

<sup>c</sup> Eg = electrochemical HOMO–LUMO energy gap.

<sup>d</sup> HOMO, LUMO energy calculated using Gaussian 03 programme at B3LYP/6-31G level.

<sup>e</sup> Computed HOMO–LUMO energy gap.

<sup>f</sup> Optical HOMO–LUMO energy gap (Zero–Zero transition energy estimated from the point of intersection of normalized absorption and emission spectra in acetonitrile).

comparable with that of the standard molecule ethidium bromide. This work provides basic understanding about the electronic properties of phenanthridine derivatives, and its spectral properties can be extended to NIR region and the work is in progress.

#### 4. Experimental section

##### 4.1. General information

All organic chemicals and solvents were purchased from Sigma Aldrich, SDFine and were used without further purification. <sup>1</sup>H and <sup>13</sup>C NMR spectra were taken on Bruker 400 MHz using CDCl<sub>3</sub> as the solvent with TMS as an internal standard. Melting points were measured on Microprocessor based melting point apparatus, and were not corrected. HRMS values were obtained on Joel GC Mate II GC-Mass Spectrometer. FTIR spectra of the synthesized organic compounds were recorded using a Jasco-4100 spectrometer instrument. UV–Visible spectra were taken using Shimadzu UV-1800 spectrophotometer. Fluorescence spectra in solution and solid states were measured using CARY-Eclipse fluorescence spectrophotometer. The fluorescence quantum yields ( $\Phi_{fl}$ ) were measured with quinine sulphate ( $\Phi_{fl}$ ) 0.546 in 0.5 N H<sub>2</sub>SO<sub>4</sub> solution as a standard,  $\lambda_{ex} = 310$  nm. Analytical Thin-layer chromatography (TLC) was performed on pre-coated plates (Merck, silica gel 60 F254). Silica gel (60–120 mesh) was used for column

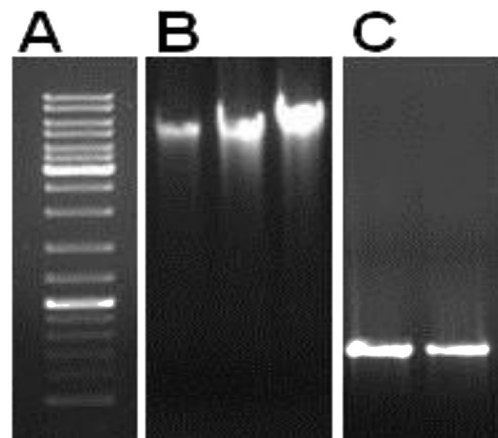


**Fig. 6.** The intercalating efficiency of compound **3** with different types of dsDNA. (A) DNA ladder with linear range of dsDNA product, (B) Bacterial genomic DNA (c) PCR product.

chromatography. Single crystal X-ray diffraction data were taken on bruker kappa APEXII. The structures were solved by direct methods. Fluorescence life time measurements were recorded using the IBH fluorescence lifetime spectrometer. Electrochemical measurements

were made using a CH instruments CH 600E electrochemical analyser. A conventional three-electrode configuration, consisting of a glassy carbon working electrode, Pt-wire counter electrode, and Ag/AgCl reference electrode, was used. 0.1 M [Bu<sub>4</sub>N]ClO<sub>4</sub> was used as supporting electrolyte.

#### 4.2. General procedure for the synthesis of 5-phenyl-7,8,13,14-tetrahydronaphthalene derivatives (**3**, **4**, **5a–5d**)

A mixture of acetaldehyde/substituted benzaldehydes (**2**) (10 mmol) and ammonium acetate (**3**) (11 mmol) was taken in a 100 ml conical flask containing 10 ml absolute ethanol at room temperature. It was sealed and warmed using water bath for 5 min until the dissolution of the solid contents. After bringing the reaction mixture to room temperature, 1 equivalent of 2-tetralone (**1**) (20 mmol) was added and sealed. Then, the mixture was warmed for 5 min and the reaction mixture was kept aside for 24 h in open air. After the completion of the reaction, as monitored by TLC, the resulting product was purified by column chromatography over silica gel (60–120 mesh) using n-hexane and ethyl acetate mixture (9:1) as eluent to give the compounds (**3**, **4**, **5a–d**). Thus, the obtained solid was further purified by recrystallizing in 1:1 ethanol and tetrahydrofuran mixture.

#### 4.3. General procedure for the synthesis of 5-phenyl-7,8,13,14-tetrahydronaphthalene-2,10-dicarbonitrile derivatives (**6a–6d**)

A mixture of 5-phenyl-7,8,13,14-tetrahydronaphthalene derivatives (1.0 mmol) and CuCN (10 mmol) in dry DMF (50 mL) was heated to reflux under N<sub>2</sub> for 72 h. The mixture was cooled to room temperature, water (100 mL) was added, and the resulting white precipitate was collected by filtration. The solid was then washed with a 30% aqueous solution of ethylenediamine until the washings were colorless. The solid was treated with dichloromethane, and the suspension was washed with 30% aqueous ethylenediamine and then with cold water, and finally with brine solution. The organic phase was dried over anhydrous MgSO<sub>4</sub> and filtered, and volatiles were then removed by evaporation under reduced pressure. Column chromatography on silica gel (petroleum ether and CH<sub>2</sub>Cl<sub>2</sub>) afforded 5-(4-phenyl)-7,8,13,14-tetrahydronaphthalene-2,10-dicarbonitrile derivatives as yellow colour solids.

##### 4.3.1. 7,8,13,14-tetrahydronaphthalene-2,10-dicarbonitrile (**3**)

White solid; Melting point: 78–80 °C; IR (KBr): 3076, 3002, 2999, 2962, 2801, 1739, 1704, 1643, 1501, 1345, 1273, 1201, 1021, 859, 832, 759, 701, 635 cm<sup>-1</sup>; <sup>1</sup>H NMR (400 MHz, CDCl<sub>3</sub>) ppm: 3.08–3.04 (t, J = 8.0 Hz, 4H), 3.20–3.17 (t, J = 6.0 Hz, 4H), 7.41–7.32 (m, 6H), 7.85–7.83 (d, J = 8.0 Hz, 2H), 8.38 (s, 1H); <sup>13</sup>C NMR (100 MHz, CDCl<sub>3</sub>) ppm: 27.5, 28.64, 29.0, 30.9, 123.5, 125.9, 126.1, 127.2, 127.3, 127.8, 127.9, 128.0, 128.2, 128.4, 128.7, 128.7, 129.0, 132.8, 136.7, 136.9, 155.6; HRMS for C<sub>21</sub>H<sub>17</sub>N Calculated [M<sup>+</sup>] m/z 283.1361, Found 283.1366.

##### 4.3.2. 5-Phenyl-7,8,13,14-tetrahydronaphthalene-2,10-dicarbonitrile (**4**)

White solid; Melting point: 223–225 °C; IR (KBr): 3066, 3034, 2960, 2929, 2831, 2326, 1737, 1544, 1487, 1425, 1396, 1290, 1089, 945, 835, 759, 744, 617 cm<sup>-1</sup>; <sup>1</sup>H NMR (400 MHz, CDCl<sub>3</sub>) ppm: 2.79–2.75 (t, J = 8.0 Hz, 2H), 2.97–2.93 (t, J = 8.0 Hz, 2H), 3.16–3.08 (m, 4H), 6.88–6.87 (d, J = 4.0 Hz, 2H), 7.13–7.09 (m, 1H), 7.36–7.24 (m, 7H), 7.46–7.43 (dd, J = 16.0, 4.0 Hz, 2H), 7.52–7.50 (d, J = 8.0 Hz, 1H); <sup>13</sup>C NMR (100 MHz, CDCl<sub>3</sub>) ppm: 29.2, 29.5, 29.6, 33.2, 125.6, 126.0, 126.9, 126.9, 127.5, 127.7, 127.8, 127.9, 128.4, 128.7, 128.8, 129.7, 129.8, 133.0, 133.1, 138.7, 139.7, 142.1, 145.7, 154.0,

158.1; HRMS for C<sub>27</sub>H<sub>21</sub>N Calculated [M<sup>+</sup>] m/z 359.1674, Found 359.1660.

##### 4.3.3. 5-(4-methoxyphenyl)-7,8,13,14-tetrahydronaphthalene-2,10-dicarbonitrile (**5a**)

Pale yellow solid; Melting point: 246–248 °C; IR (KBr): 3049, 3032, 2993, 2900, 2833, 2326, 1745, 1604, 1543, 1508, 1396, 1290, 1230, 1105, 1029, 879, 833, 746, 717, 586 cm<sup>-1</sup>; <sup>1</sup>H NMR (400 MHz, CDCl<sub>3</sub>) ppm: 2.77–2.74 (t, J = 6.0 Hz, 2H), 2.95–2.92 (t, J = 6.0 Hz, 2H), 3.08–3.06 (t, J = 4.0 Hz, 2H), 3.13–3.09 (t, J = 8.0 Hz, 2H), 3.82 (s, 3H), 6.87–6.85 (d, J = 8.0 Hz, 2H), 6.93–6.89 (t, J = 8.0 Hz, 1H), 6.97–6.95 (d, J = 8.0 Hz, 1H), 7.13–7.09 (t, J = 8.0 Hz, 1H), 7.35–7.23 (m, 4H), 7.40–7.38 (d, J = 8.0, 2H), 7.50–7.48 (d, J = 8.0, 1H); <sup>13</sup>C NMR (100 MHz, CDCl<sub>3</sub>) ppm: 29.3, 29.5, 29.6, 33.2, 55.3, 113.8, 125.7, 126.0, 126.8, 127.1, 127.5, 127.8, 128.6, 128.7, 129.5, 131.1, 133.2, 133.3, 134.5, 138.7, 139.6, 145.7, 153.6, 158.1, 159.4; HRMS for C<sub>28</sub>H<sub>23</sub>NO Calculated [M<sup>+</sup>] m/z 389.1780, Found 389.1780.

##### 4.3.4. N,N-dimethyl-4-(7,8,13,14-tetrahydronaphthalene-2,10-dicarbonitrile-5-yl)aniline (**5b**)

Yellow solid; Melting point: 216–218 °C; IR (KBr): 3053, 3017, 2937, 2829, 2326, 1764, 1579, 1506, 1454, 1392, 1361, 1230, 1123, 997, 943, 742, 673, 663 cm<sup>-1</sup>; <sup>1</sup>H NMR (400 MHz, CDCl<sub>3</sub>) ppm: 2.77–2.74 (t, J = 6.0 Hz, 2H), 2.95–2.92 (t, J = 6.0 Hz, 2H), 3.96 (s, 6H), 3.08–3.06 (t, J = 4.0 Hz, 2H), 3.13–3.09 (t, J = 8.0 Hz, 2H), 6.68–6.66 (d, J = 8.0 Hz, 2H), 6.96–6.92 (t, J = 8.0 Hz, 1H), 7.13–7.08 (m, 2H), 7.35–7.23 (m, 6H), 7.50–7.48 (d, J = 8.0, 1H); <sup>13</sup>C NMR (100 MHz, CDCl<sub>3</sub>) ppm: 29.3, 29.6, 29.6, 33.2, 40.5, 112.2, 125.6, 125.9, 126.5, 126.6, 126.7, 127.3, 127.8, 128.2, 128.6, 129.5, 130.0, 130.8, 133.3, 133.7, 138.5, 139.6, 145.6, 150.3, 154.2, 158.0; HRMS for C<sub>29</sub>H<sub>26</sub>N<sub>2</sub> Calculated [M<sup>+</sup>] m/z 402.2096, Found 402.2090.

##### 4.3.5. N,N-diethyl-4-(7,8,13,14-tetrahydronaphthalene-2,10-dicarbonitrile-5-yl)aniline (**5c**)

Yellow solid; Melting point: 178–180 °C; IR (KBr): 3059, 3027, 2968, 2893, 2835, 2326, 1712, 1606, 1517, 1427, 1398, 1371, 1267, 1195, 1180, 1076, 1006, 798, 746, 623 cm<sup>-1</sup>; <sup>1</sup>H NMR (400 MHz, CDCl<sub>3</sub>) ppm: 1.17–1.13 (t, J = 8.0 Hz, 6H), 2.77–2.74 (t, J = 6.0 Hz, 2H), 2.95–2.92 (t, J = 6.0 Hz, 2H), 3.12–3.06 (m, 4H), 3.39–3.33 (q, J = 8.0 Hz, 4H), 6.63–6.61 (d, J = 8.0 Hz, 2H), 6.96–6.92 (t, J = 8.0 Hz, 1H), 7.16–7.09 (m, 2H), 7.34–7.23 (m, 6H), 7.50–7.48 (d, J = 8.0, 1H); <sup>13</sup>C NMR (100 MHz, CDCl<sub>3</sub>) ppm: 12.6, 29.3, 29.6, 29.6, 33.3, 44.4, 111.7, 125.6, 125.9, 126.4, 126.6, 126.7, 127.3, 127.8, 128.1, 128.6, 128.8, 129.5, 130.9, 133.4, 133.9, 138.5, 139.6, 145.6, 147.6, 154.3, 158.0; HRMS for C<sub>31</sub>H<sub>30</sub>N<sub>2</sub> Calculated [M<sup>+</sup>] m/z 430.2409, Found 430.2400.

##### 4.3.6. 5-(4-nitrophenyl)-7,8,13,14-tetrahydronaphthalene-2,10-dicarbonitrile (**5d**)

Yellow solid; Melting point: 230–232 °C; IR (KBr): 3051, 3021, 2947, 2883, 2841, 2326, 1745, 1691, 1593, 1556, 1508, 1394, 1340, 1290, 1132, 765, 744, 663 cm<sup>-1</sup>; <sup>1</sup>H NMR (400 MHz, CDCl<sub>3</sub>) ppm: 2.82–2.79 (t, J = 6.0 Hz, 2H), 2.99–2.96 (t, J = 6.0 Hz, 2H), 3.10–3.07 (t, J = 6.0 Hz, 2H), 3.19–3.16 (t, J = 6.0 Hz, 2H), 6.80–6.78 (d, J = 8.0 Hz, 1H), 6.94–6.90 (t, J = 8.0 Hz, 1H), 7.20–7.16 (t, J = 8.0 Hz, 1H), 7.39–7.26 (m, 4H), 7.54–7.52 (d, J = 8.0, 1H), 7.66–7.64 (d, J = 8.0 Hz, 2H), 8.21–8.19 (d, J = 8.0 Hz, 2H); <sup>13</sup>C NMR (100 MHz, CDCl<sub>3</sub>) ppm: 29.1, 29.4, 29.5, 33.1, 123.6, 126.0, 126.2, 127.3, 127.7, 128.0, 128.1, 128.5, 128.8, 129.5, 129.6, 130.9, 132.1, 132.6, 138.9, 139.7, 146.11, 147.28, 148.7, 151.1, 158.6; HRMS for C<sub>27</sub>H<sub>20</sub>N<sub>2</sub>O<sub>2</sub> Calculated [M<sup>+</sup>] m/z 404.1525, Found 404.1526.

##### 4.3.7. 5-(4-methoxyphenyl)-7,8,13,14-tetrahydronaphthalene-2,10-dicarbonitrile (**6a**)

Pale yellow solid; Melting point: 218–220 °C; IR (KBr): 3047, 3022, 3001, 2983, 2900, 2854, 2327, 1755, 1607, 1547, 1501, 1386,

1295, 1230, 1115, 1039, 897, 833, 749, 714, 645, 576 cm<sup>-1</sup>; <sup>1</sup>H NMR (400 MHz, CDCl<sub>3</sub>) ppm: 2.78–2.75 (t, *J* = 6.0 Hz, 2H), 2.94–2.90 (t, *J* = 8.0 Hz, 2H), 3.05–3.02 (m, 4H), 3.78 (s, 3H), 6.83–6.81 (d, *J* = 8.0 Hz, 2H), 6.99–6.97 (d, *J* = 8.0 Hz, 1H), 7.16–7.13 (dd, *J* = 16.0, 4.0 Hz, 1H), 7.31–7.25 (m, 2H), 7.56–7.48 (m, 4H); <sup>13</sup>C NMR (100 MHz, CDCl<sub>3</sub>) ppm: 14.1, 28.9, 29.7, 55.4, 114.2, 128.9, 129.5, 130.0, 130.6, 131.2, 160.2; HRMS for C<sub>30</sub>H<sub>21</sub>N<sub>3</sub>O Calculated [M<sup>+</sup>] *m/z* 439.1685, Found 439.1690.

#### 4.3.8. 5-(4-(dimethylamino)phenyl)-7,8,13,14-tetrahydrodibenzo[a,i]phenanthridine-2,10-dicarbonitrile (**6b**)

Yellow solid; Melting point: 216–218 °C; IR (KBr): 3066, 3010, 2951, 2900, 2888, 2857, 2329, 1759, 1504, 1499, 1464, 1431, 1429, 1390, 1301, 1214, 1105, 1088, 955, 801, 741 cm<sup>-1</sup>; <sup>1</sup>H NMR (400 MHz, CDCl<sub>3</sub>) ppm: 2.66–2.63 (t, *J* = 6.0 Hz, 2H), 2.82–2.79 (t, *J* = 6.0 Hz, 2H), 2.88 (s, 6H), 2.96–2.93 (m, 4H), 6.58–6.56 (d, *J* = 8.0 Hz, 2H), 6.83–6.81 (d, *J* = 8.0 Hz, 1H), 6.96–6.94 (d, *J* = 8.0 Hz, 1H), 7.29–7.19 (m, 3H), 7.33–7.29 (m, 2H), 7.39 (s, 1H); <sup>13</sup>C NMR (100 MHz, CDCl<sub>3</sub>) ppm: 23.7, 23.9, 27.5, 34.2, 106.8, 115.2, 123.4, 123.7, 124.3, 124.6, 125.3, 125.6, 135.2, 136.3, 145.1, 152.2; HRMS for C<sub>31</sub>H<sub>24</sub>N<sub>4</sub> Calculated [M<sup>+</sup>] *m/z* 452.2001, Found 452.2020.

#### 4.3.9. 5-(4-(diethylamino)phenyl)-7,8,13,14-tetrahydrodibenzo[a,i]phenanthridine-2,10-dicarbonitrile (**6c**)

Yellow solid; Melting point: 212–214 °C; IR (KBr): 3109, 3017, 2974, 2960, 2838, 2333, 1885, 1756, 1636, 1539, 1477, 1423, 1389, 1350, 1228, 1197, 1169, 1085, 999, 851, 831, 619, 588 cm<sup>-1</sup>; <sup>1</sup>H NMR (400 MHz, CDCl<sub>3</sub>) ppm: 1.14–1.10 (t, *J* = 8.0 Hz, 3H), 2.76–2.73 (t, *J* = 6.0 Hz, 2H), 2.90–2.88 (m, 4H), 3.08–3.04 (t, *J* = 6.0 Hz, 2H), 3.38–3.34 (q, *J* = 4.0 Hz, 2H), 6.61–6.59 (d, *J* = 8.0 Hz, 2H), 6.94–6.92 (d, *J* = 8.0 Hz, 1H), 7.11–7.09 (d, *J* = 8.0 Hz, 1H), 7.21–7.19 (d, *J* = 8.0 Hz, 2H), 7.50–7.46 (t, *J* = 8.0 Hz, 3H), 7.59 (s, 1H); <sup>13</sup>C NMR (100 MHz, CDCl<sub>3</sub>) ppm: 12.3, 28.3, 28.5, 32.4, 38.9, 43.6, 110.7, 119.7, 126.5, 127.4, 128.1, 128.8, 129.5, 130.2, 130.3, 130.4, 130.7, 131.8, 132.6, 140.9, 141.5, 145.1, 147.2, 157.3; HRMS for C<sub>33</sub>H<sub>28</sub>N<sub>4</sub> Calculated [M<sup>+</sup>] *m/z* 480.2314, Found 480.2315.

#### 4.3.10. 5-(4-nitrophenyl)-7,8,13,14-tetrahydrodibenzo[a,i]phenanthridine-2,10-dicarbonitrile (**6d**)

Yellow solid; Melting point: 208–210 °C; IR (KBr): 3110, 3011, 2984, 2875, 2812, 1783, 1537, 1471, 1388, 1345, 1210, 1171, 1148, 1102, 1095, 1066, 870, 827, 793, 636; <sup>1</sup>H NMR (400 MHz, CDCl<sub>3</sub>) ppm: 2.61–2.58 (t, *J* = 6.0 Hz, 2H), 2.77–2.74 (t, *J* = 6.0 Hz, 2H), 2.93–2.86 (m, 4H), 6.47–6.45 (d, *J* = 8.0 Hz, 1H), 6.89–6.87 (d, *J* = 8.0 Hz, 1H), 7.08 (s, 1H), 7.19–7.17 (d, *J* = 8.0 Hz, 1H), 7.29–7.27 (d, *J* = 8.0 Hz, 1H), 7.34 (s, 1H), 7.40–7.38 (d, *J* = 8.0 Hz, 2H), 7.48–7.46 (d, *J* = 8.0 Hz, 2H); <sup>13</sup>C NMR (100 MHz, CDCl<sub>3</sub>) ppm: 23.5, 23.8, 23.9, 27.5, 106.5, 116.4, 116.8, 122.4, 123.3, 123.9, 124.1, 124.8, 125.0, 125.3, 125.6, 125.7, 125.8, 126.2, 127.0, 135.5, 136.5, 140.3, 140.8, 153.2; HRMS for C<sub>29</sub>H<sub>18</sub>N<sub>4</sub>O<sub>2</sub> Calculated [M<sup>+</sup>] *m/z* 454.1430, Found 454.1431.

#### 5. Agarose gel electrophoresis

A 5 μl aliquots of different concentration of genomic DNA, polymerase chain reaction amplified DNA and Gene Ruler DNA ladder mix (Thermo scientific, USA) were electrophoresed on a 0.8% agarose gel in 1× TAE buffer at 50 V for 45 min, stained with compound **3** to **6d**, and visualized with a UV transilluminator. The images were captured with a Syngene GBoxGelDoc System.

#### Author contributions

The manuscript was written through contributions of all authors.

#### Acknowledgements

B.U thanks CSIR for providing Senior Research Fellowship (CSIR-SRF, Acknowledgement No-09/844(0018)/2013EMR-I). S. E and U. S thank DST (Grant No.SERB/F/4232/2013-15) India. The work is also supported by CSIR supraregional, XIIth five year plan project STRAIT. We also thank VIT-SIF, NCUFP-University of Madras, and SAIF-IIT Madras for NMR, lifetime and single crystal X-ray diffraction facilities respectively. The authors thank Dr. R. Srinivasan, SSL-VIT for language editing.

#### Appendix A. Supplementary data

Supplementary data related to this article can be found at <http://dx.doi.org/10.1016/j.dyepig.2016.07.036>.

#### References

- Zhang B, Studer A. Recent advances in the synthesis of nitrogen heterocycles via radical cascade reactions using isonitriles as radical acceptors. *Chem Soc Rev* 2015;44:3505–21.
- Nakanishi T, Suzuki M, Mashiba A, Ishikawa K, Yokotsuka T. Synthesis of NK109, an anticancer benzo[c]phenanthridine alkaloid. *J Org Chem* 1998;63: 4235–9.
- Chen J-J, Li K-T, Yang D-Y. Synthesis of coumarin/phenanthridine-fused heterocycles and their photochemical and thermochromic properties. *Org Lett* 2011;13:1658–61.
- Lv P, Huang X, Xie L, Xu X. Palladium-catalyzed tandem reaction to construct benzo[c]phenanthridine: application to the total synthesis of benzo [c] phenanthridine alkaloids. *Org Biomol Chem* 2011;9:3133–5.
- Jiang H, Cheng Y, Wang R, Zheng M, Zhang Y, Yu S. Synthesis of 6-Alkylated phenanthridine derivatives using photoredox neutral somophilic isocyanide insertion. *Angew Chem Int Ed* 2013;52:13289–92.
- Berg S-S. The search for new trypanocides. Part VIII. Coupling of m-amidobenzenediazonium chloride with 3,8-diamino-5-ethyl-6-phenylphenanthridinium chloride. *J Chem Soc* 1963;3635–40.
- Henderson J-F. Inhibition of purine metabolism in ehrlich ascites carcinoma cells by phenanthridinium compounds related to ethidium bromide. *Cancer Res* 1963;23:491.
- Nandi S, Routh P, Layek R-K, Nandi A-K. Ethidium bromide-adsorbed graphene templates as a platform for preferential sensing of DNA. *Biomacromolecules* 2012;13:3181–8.
- Tam V-K, Liu Q, Tor Y. Extended ethidium bromide analogue as a triple helix intercalator: synthesis, Photophysical properties and nucleic acids binding. *Chem Commun* 2006:2684–6.
- Nakamura M, Awaad A, Hayashi K, Ochiai K, Ishimura K. Thiol-organosilica particles internally functionalized with propidium iodide as a multicolor fluorescence and x-ray computed tomography probe and application for non-invasive functional gastrointestinal tract imaging. *Chem Mater* 2012;24: 3772–9.
- Sanju K-S, Thurakkal S, Neelakandan P-P, Joseph J, Ramaiah D. Simultaneous binding of a cyclophane and classical intercalators to DNA: observation of FRET-mediated white light emission. *Phys Chem Chem Phys* 2015;17: 13495–500.
- Samanta A, Paul B-K, Guchhait N. Photophysics of DNA staining dye Propidium Iodide encapsulated in bio-mimetic micelle and genomic fish sperm DNA. *J Photochem Photobiol B* 2012;109:58–67.
- Yan L, Zhao D, Lan J, Cheng Y, Guo Q, Li X, et al. Palladium-catalyzed tandem N–H/C–H arylation: regioselective synthesis of N-heterocycle-fused phenanthridines as versatile blue-emitting luminophores. *Org Biomol Chem* 2013;11:7966–77.
- Wainwright M. Dyes in the development of drugs and pharmaceuticals. *Dyes Pigments* 2008;76:582–9.
- Piechowska J, Gryko D-T. Preparation of a family of 10-Hydroxybenzo[h]quinoline analogues via a modified sandford reaction and their excited state intramolecular proton transfer properties. *J Org Chem* 2011;76:10220–8.
- Robaa D, Enzensperger C, Azm S-E-D-A, Khawass E-S-E, Sayed O-E, Lehmann J. Dopamine receptor ligands. Part 18:(1) modification of the structural skeleton of indolobenzazecine-type dopamine receptor antagonists. *J Med Chem* 2010;53:2646–50.
- Chen Y-F, Wu Y-S, Jhan Y-H, Hsieh J-C. An efficient synthesis of (NH)-phenanthridinones via ligand-free copper-catalyzed annulations. *Org Chem Front* 2014;1:253–7.
- Cairns A-G, Senn H-M, Murphy M-P, Hartley R-C. Expanding the palette of phenanthridinium cations. *Chem Eur J* 2014;20:3742–51.
- Duarte T-M-F, Müllen K. Pyrene-based materials for organic electronics. *Chem Rev* 2011;111:7260–314.
- Lin Y, Li Y, Zhan X. Small molecule semiconductors for high-efficiency organic photovoltaics. *Chem Soc Rev* 2012;41:4245–72.

- [21] Ramkumar V, Kannan P. Highly fluorescent semiconducting pyrazoline materials for optoelectronics. *Opt Mater* 2015;46:605–13.
- [22] Wu J, Lai G, Li Z, Lu Y, Leng T, Shen Y, et al. Novel 2,1,3-benzothiadiazole derivatives used as selective fluorescent and colorimetric sensors for fluoride ion. *Dyes Pigments* 2016;124:268–76.
- [23] Liu Z, Peng C, Guo C, Zhao Y, Yang X, Pei M, et al. Novel fluorescent and colorimetric pH sensors derived from benzimidazo[2,1-*a*]benz[*d*]isoquinoline-7-one-12-carboxylic acid. *Tetrahedron* 2015;71:2736–42.
- [24] Shanmugaraju S, Mukherjee P-S.  $\pi$ -Electron rich small molecule sensors for the recognition of nitroaromatics. *Chem Commun* 2015;51:16014–32.
- [25] Schäferling M. The art of fluorescence imaging with chemical sensors. *Angew Chem Int Ed* 2012;51:3532–54.
- [26] Xu J, Li Q, Yue Y, Guo Y, Shao S. A water-soluble BODIPY derivative as a highly selective “Turn-On” fluorescent sensor for  $H_2O_2$  sensing *in vivo*. *Biosens Bioelectron* 2014;56:58–63.
- [27] Schutting S, Borisov S-M, Klimant I. Diketo-Pyrrolo-pyrrole dyes as new colorimetric and fluorescent pH indicators for optical carbon dioxide sensors. *Anal Chem* 2013;85:3271–9.
- [28] Sudharsanam R, Chandrasekaran S, Das P-K. Unsymmetrical aryl disulfides with excellent transparency in the visible region for second order nonlinear optics. *J Mater Chem* 2002;12:2904–8.
- [29] Umamahesh B, Sathianarayanan K-I. Synthesis and optical properties of a series of green-light-emitting 2-(4-Phenylquinolin-2-yl)phenol–BF<sub>2</sub> complexes (boroquinols). *Eur J Org Chem* 2015;5089–98.
- [30] Frederickson C-K, Haley M-M. Synthesis and optoelectronic properties of indeno[1,2-*b*]fluorene-6,12-dione donor–acceptor–donor triads. *J Org Chem* 2014;79:11241–5.
- [31] Easwaramoorthi S, Umamahesh B, Cheranmadeni P, Rathorec R-S, Sathianarayanan K-I. Synthesis of green light emitting fused pyrazolinopiperidines – photophysical and electrochemical studies. *RSC Adv* 2013;3:1243–54.
- [32] Pamuk M, Algi F. Incorporation of a 2, 3-dihydro-1*H*-pyrrolo[3,4-*d*]pyridazine-1,4(6*H*)-dione unit into a donor–acceptor triad: synthesis and ion recognition features. *Tetrahedron Lett* 2012;53:7117–20.
- [33] Umamahesh B, Triveni R-M, Sathianarayanan K-I. A novel, facile, rapid, solvent free protocol for the one pot green synthesis of chromeno[2,3-*d*]pyrimidines using reusable nano ZnAl<sub>2</sub>O<sub>4</sub> – a NOSE approach and photophysical studies. *RSC Adv* 2015;5:6578–87.
- [34] Umamahesh B, Sathianarayanan K-I. CuO–CuAl<sub>2</sub>O<sub>4</sub> and d-glucose catalyzed synthesis of a family of excited state intramolecular proton transfer imidazo [1, 2-*a*] pyridine analogues and their optical properties. *Dyes Pigments* 2015;12:88–98.
- [35] Xu Z, Singh N-J, Lim J, Pan J, Kim H-N, Park S, et al. Unique sandwich stacking of pyrene–adenine–pyrene for selective and ratiometric fluorescent sensing of ATP at physiological P<sup>H</sup>. *J Am Chem Soc* 2009;131:15528–33.
- [36] Yang L, Liu Y, Zhou X, Wu Y, Ma C, Liu W, et al. Asymmetric anthracene-fused BODIPY dye with large Stokes shift: synthesis, photophysical properties and bioimaging. *Dyes Pigments* 2016;126:232–8.
- [37] Hung W-I, Liao Y-Y, Hsu C-Y, Chou H-H, Lee T-H, Kao W-S, et al. High-performance dye-sensitized solar cells based on phenothiazine dyes containing double anchors and thiophene spacers. *Chem Asian J* 2014;9:357–66.
- [38] Sathianarayanan K, Karthikeyan N-S, Aravindan P-G, Shanthi S, Rathore R, Lee C-W. Dual behavior of 2-tetralone: a new approach for the synthesis of 5-aryl-7,8,13,14-tetrahydrodibenzo[*a,i*]phenanthridine. *J Heterocycl Chem* 2009;46:1142–4.
- [39] Umamahesh B, Sathiskumar U, Easwaramoorthi S, Sathianarayanan K. Synthesis, photophysical and acidochromic properties of a series of tetrahydrodibenzo[*a,i*]phenanthridine chromophores. *Dyes Pigments* 2016;130: 233–44.
- [40] Lippert E. *Z Naturforsch A* 1955;10:541.
- [41] Frisch MJ, Trucks GW, Schlegel HB, Scuseria GE, Robb JR MA, et al. Gaussian 03 rev. E01. Wallingford CT: Gaussian, inc.; 2004.